26. James, P., Vorherr, T. & Carafoli, E. Calmodulin-binding domains: just two-faced or multi-faceted? *Trends Biochem. Sci.* **20,** 38–42 (1995).
27. Fletcher, C. F. *et al.* Absence epilepsy in tottering mutant mice is associated with calcium channel defects. *Cell* **87,** 607–617 (1996).
28. Harper, J. W., Adami, G. R., Wei, N., Keyomarsi, K. & Elledge, S. J. The p21 Cdk-interacting protein Cip1 is a potent inhibitor of G1 cyclin-dependent kinases. *Cell* **75,** 805–816 (1993).
29. Sakurai, T., Westenbroek, R. E., Rettig, J., Hell, J. & Catterall, W. A. Biochemical properties and subcellular distribution of the BI and rbA isoforms of α_{1A} subunits of brain calcium channels. *J. Cell. Biol.* **134,** 511–528 (1996).
30. Yokoyama, C. T., Sheng, Z.-H. & Catterall, W. A. Phosphorylation of the synaptic protein interaction site on N-type calcium channels inhibits interactions with SNARE proteins. *J. Neurosci.* **17,** 6929–6938 (1997).

Acknowledgements. We thank T. Snutch, M. Harpold and K. Campbell for cDNAs encoding Ca^{2+}-channel subunits. This work was supported by an NRSA postdoctoral fellowship from the NIH to A.L. and by research grants from the NIH to D.R.S. and W.A.C.

Correspondence and requests for materials should be addressed to W.A.C. (e-mail: wcatt@u.washington.edu).

Calmodulin supports both inactivation and facilitation of L-type calcium channels

Roger D. Zühlke*†, Geoffrey S. Pitt†‡§, Karl Deisseroth§, Richard W. Tsien§ & Harald Reuter*

** Department of Pharmacology, University of Bern, 3010 Bern, Switzerland*
‡ Division of Cardiovascular Medicine and § Department of Molecular and Cellular Physiology, Stanford University Medical School, Stanford, California 94305-5426, USA
† These authors contributed equally to this work.

L-type Ca^{2+} channels support Ca^{2+} entry into cells, which triggers cardiac contraction[1], controls hormone secretion from endocrine cells[2] and initiates transcriptional events that support learning and memory[3]. These channels are examples of molecular signal-transduction units that regulate themselves through their own activity. Among the many types of voltage-gated Ca^{2+} channel, L-type Ca^{2+} channels particularly display inactivation and facilitation, both of which are closely linked to the earlier entry of Ca^{2+} ions[4–10]. Both forms of autoregulation have a significant impact on the amount of Ca^{2+} that enters the cell during repetitive activity, with major consequences downstream. Despite extensive biophysical analysis[9], the molecular basis of autoregulation remains unclear, although a putative Ca^{2+}-binding EF-hand motif[11,12] and a nearby consensus calmodulin-binding isoleucine-glutamine ('IQ') motif[13,14] in the carboxy terminus of the α_{1C} channel subunit have been implicated[12,14–16]. Here we show that calmodulin is a critical Ca^{2+} sensor for both inactivation and facilitation, and that the nature of the modulatory effect depends on residues within the IQ motif important for calmodulin binding. Replacement of the native isoleucine by alanine removed Ca^{2+}-dependent inactivation and unmasked a strong facilitation; conversion of the same residue to glutamate eliminated both forms of autoregulation. These results indicate that the same calmodulin molecule may act as a Ca^{2+} sensor for both positive and negative modulation.

Deletion of the first eight amino acids of the IQ motif in the C-terminal tail of the Ca^{2+}-channel subunit α_{1C} (Fig. 1a) eliminates Ca^{2+}-dependent inactivation[14], but there is no information about any interaction with calmodulin (CaM) or its functional role in Ca^{2+}-dependent inactivation or facilitation. Mutation of the isoleucine residue Ile 1624 to alanine, valine or glutamate (77I/A, 77I/V, 77I/E; Fig. 1b) revealed that this amino acid has a critical role in Ca^{2+}-dependent inactivation and facilitation. Complementary RNAs (cRNAs) for wild-type α_{1C} (77WT)[14,17] or its mutants were injected into *Xenopus* oocytes, together with cRNAs for the auxiliary subunits $\alpha_2\delta$ and β_1. Both Ba^{2+} and Ca^{2+} currents (I_{Ba} and I_{Ca}) through the expressed channels were recorded in every oocyte (representative traces are shown in Fig. 1c). As reported[14], channel 77WT shows prominent Ca^{2+}-dependent inactivation. In contrast, channel mutants 77I/A and 77I/E did not show this type of inactivation. In fact, the decay of I_{Ca} through 77I/A was sometimes even slightly slower than that of I_{Ba}. However, channel 77I/V showed Ca^{2+}-dependent inactivation similar to that of 77WT (Fig. 1c). Data were pooled using the ratio of the current values at 400 ms and at the initial peak (r_{400}, Fig. 1d) as an index of inactivation. The residual current fraction (r_{400}) for Ca^{2+} was significantly smaller than that for Ba^{2+} for both 77WT and 77I/V, but not for 77I/A and 77I/E.

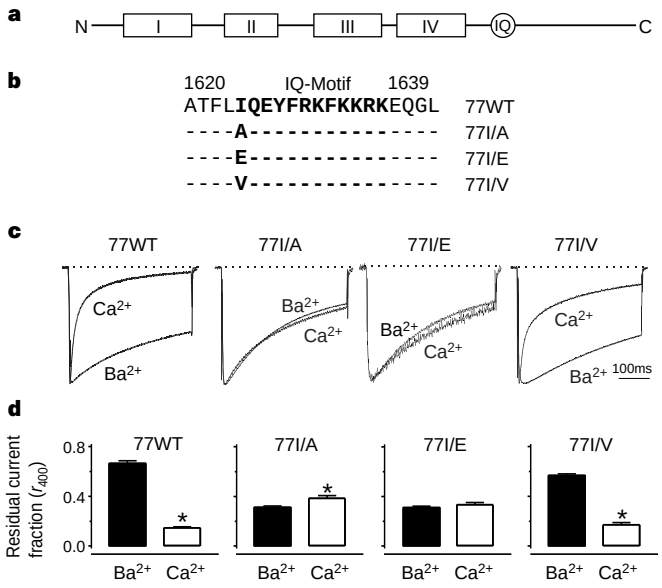

Figure 1 Point mutations in the IQ motif of 77WT affect Ca^{2+}-dependent inactivation. **a**, 77WT with four transmembrane domains (I–IV) and a consensus CaM-binding IQ motif 148 amino acids downstream of transmembrane segment S6 in domain IV. **b**, Sequence alignment of amino acids 1,620–1,639 of 77WT (IQ motif in bold) and its variants with the respective point mutations at position 1,624. **c**, Representative currents recorded from 77WT and its mutants during test-pulses of V_h from –90 to +20 mV. I_{Ca} was scaled to peak I_{Ba}. **d**, Residual fractions of peak currents remaining at the end of a 400-ms test-pulse (r_{400}), plotted for I_{Ba} and I_{Ca} supported by 77WT, 77I/A, 77I/E and 77I/V (n = 8–20 each). Asterisk, $P < 0.001$ vs. I_{Ba}, paired t-test.

Unexpectedly, mutations at amino-acid residue position 1,624 also influenced Ca^{2+}-dependent facilitation during trains of voltage pulses (Fig. 2). Ca^{2+} currents supported by 77I/A increased markedly with repeated depolarizations to +20 mV, whereas Ba^{2+} currents increased very little (Fig. 2a, b). This can be seen in records of I_{Ca} and I_{Ba} (Fig. 2a), scaled according to their peak amplitudes at the basal frequency of stimulation (0.1 Hz) to allow for intrinsic differences in open channel flux[18]. Peak I_{Ca} showed increasingly strong facilitation as pulse frequency was raised, reaching 72% above baseline at 3.3 Hz, but peak I_{Ba} increased only marginally at higher frequencies. The facilitation was an incremental phenomenon, as illustrated with trains of 40 pulses (Fig. 2b). In contrast to 77I/A, 77WT and mutant channels 77I/E and 77I/V exhibited little or no overt potentiation at any frequency between 0.5 and 3.3 Hz, with either Ca^{2+} or Ba^{2+} as charge carriers (Fig. 2c).

Might the strong facilitation observed with mutant 77I/A be a general channel property that is sometimes masked by Ca^{2+}-dependent inactivation? We used a two-pulse protocol to look in more detail at the kinetics of recovery from the effects of an initial conditioning pulse (Fig. 3). The pattern of differences between I_{Ba} and I_{Ca} varied strikingly, depending on the amino acid at position 1,624. In 77WT (and in 77I/V), the Ca^{2+}-dependence of inactivation was manifested by a lesser degree of recovery with Ca^{2+} than with Ba^{2+} as charge carrier, seen over the first ~30 ms of recovery[14]. At later times, however, the differential reversed, with faster recovery

© 1999 Macmillan Magazines Ltd

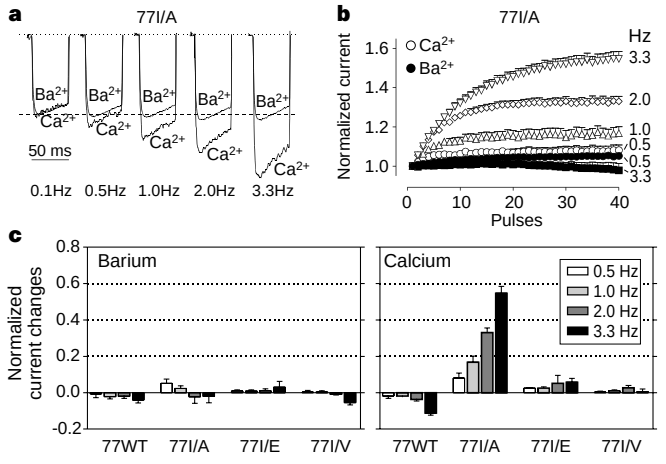

Figure 2 Frequency-dependent facilitation of I_{Ca} conducted by 77I/A. **a**, I_{Ba} and I_{Ca} current traces taken at the end of trains of 40 test pulses of V_h from –90 to +20 mV, at 0.1 to 3.3 Hz. I_{Ba} and I_{Ca} traces were normalized to their respective scaled amplitude at 0.1 Hz (dashed line). **b**, Peak I_{Ba} (filled symbols) and I_{Ca} (open symbols) during trains of 40 repetitive test-pulses at 0.1–3.3 Hz were normalized to the current amplitude at the beginning of each train. **c**, Changes in peak I_{Ba} (left panel) and I_{Ca} (right panel) conducted by 77WT, 77I/A, 77I/E and 77I/V (n = 4–12 each) at indicated stimulation frequencies. Note that frequency-dependent facilitation was present only in 77I/A.

for I_{Ca}. In contrast, with 77I/A, I_{Ca} recovered faster than I_{Ba} at all times, reaching a peak value 20% greater than that during the first pulse after a rest period of >200 ms. For 77I/E, recovery of I_{Ca} and I_{Ba} was rapid and indistinguishable at all recovery intervals. These results indicate that the amino acids at position 1,624 are critical for both early and late differences. The late differences can be interpreted as facilitation, which can be observed in combination with Ca^{2+}-dependent inactivation (77WT and 77I/V), in isolation (77I/A), or not at all (77I/E).

As isoleucine is the first amino acid in the putative CaM-binding IQ motif in 77WT and its mutation had such a profound effect on the channel's Ca^{2+}-sensitive feedback mechanisms, we tested whether binding of CaM to the IQ motif could be involved in the regulation of Ca^{2+}-dependent inactivation and facilitation.

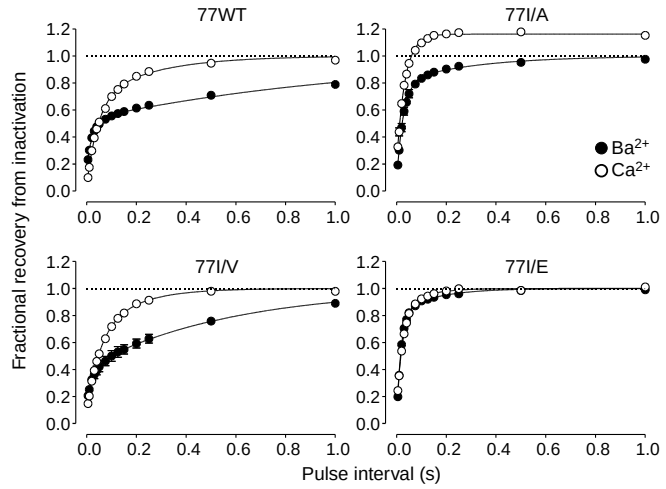

Figure 3 Repriming experiments reveal Ca^{2+}-dependent facilitation of 77WT and 77I/V. Recovery from inactivation of I_{Ba} and I_{Ca} was studied with a standard two-pulse protocol. During prepulses of V_h from –90 to +20 mV, currents were reduced to 15–20%, and subsequent test pulses applied at variable intervals after prepulses revealed the kinetics of recovery from inactivation. Fractional recovery of peak I_{Ba} and I_{Ca} for 77WT and its mutants are plotted against the interpulse interval. Solid lines represent averaged bi-exponential fits of 4–7 experiments.

Although previous experiments have failed to demonstrate any effect of the CaM inhibitor calmidazolium on Ca^{2+}-dependent inactivation[9,14], a role for CaM would not be ruled out by these experiments if CaM was protected from calmidazolium at basal Ca^{2+} concentrations[19]. Accordingly, we tested the effects of a CaM mutant (here called CaM(3–)) that contained alanine instead of aspartate in three out of the four Ca^{2+}-binding EF-hand motifs[19]. When CaM(WT) was co-expressed with Ca^{2+}-channel subunits in oocytes, there was little effect on the pattern of inactivation of I_{Ba} and I_{Ca} (Fig. 4) compared to controls lacking exogenous CaM (Fig. 1c, d). However, CaM(3–) strongly inhibited Ca^{2+}-dependent inactivation of channels 77WT and 77I/V (Fig. 4a, b) and also completely eliminated Ca^{2+}-dependent facilitation of I_{Ca} through channel 77I/A (Fig. 4c, d). There was no effect on facilitation after the injection of cRNA for CaM(WT) (Fig. 4c, d). These results demonstrate that CaM plays a pivotal role in both Ca^{2+}-dependent inactivation and facilitation.

Having found that amino-acid alterations within the conserved IQ motif cause significant changes in Ca^{2+}-dependent plasticity of channel function, and having demonstrated that CaM is involved, we investigated whether CaM binds to the channel motif in a channel-specific manner. We first examined whether CaM binds to the entire α_{1C}-cytoplasmic tail (Fig. 5a). A ^{35}S-labelled *in vitro*-translated α_{1C}-cytoplasmic tail did bind to immobilized CaM in the presence of saturating Ca^{2+}, but not in the absence of Ca^{2+}. Mutating Ile 1624 to glutamate, which extinguished the CaM-dependent inactivation and facilitation in the native channel, decreased CaM binding more than 5-fold (Fig. 5a). Ca^{2+}-dependent interactions were examined in experiments using a 20-amino-acid peptide encompassing the IQ region of 77WT (α_{1C} in Fig. 5b). We tested for possible binding between the peptide and CaM in gel-shift assays

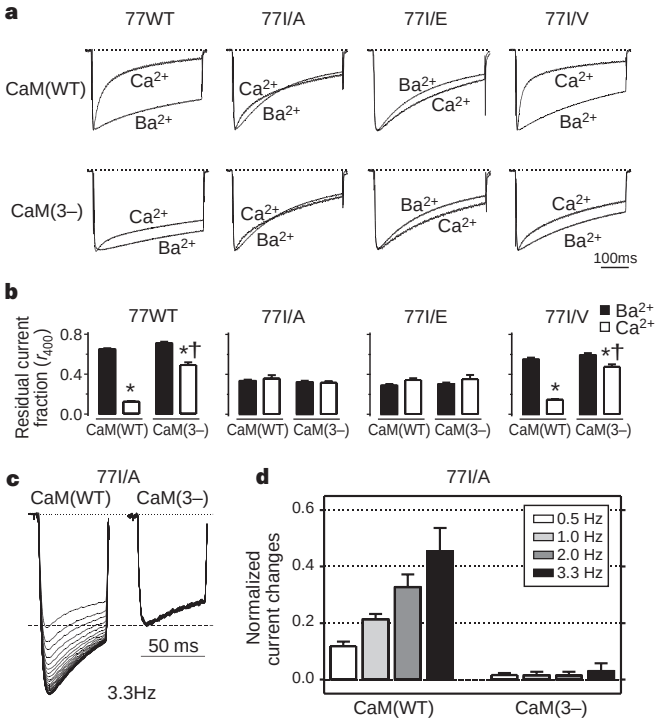

Figure 4 A mutant calmodulin, CaM(3–), inhibits Ca^{2+}-dependent inactivation and facilitation. **a**, I_{Ba} and scaled I_{Ca} traces recorded from oocytes expressing 77WT or its mutants together with CaM(WT) (upper panel) or CaM(3–) (lower panel). **b**, Differences between r_{400} values of I_{Ca} and I_{Ba} through 77WT and 77I/V (n = 6–16) were pronounced with CaM(WT), but reduced with CaM(3–); no significant differences in 77I/A and 77I/E (n = 4–10). **c**, Co-expression of 77I/A with CaM(3–), but not with CaM(WT), eliminated I_{Ca} facilitation with repetitive pulsing. **d**, Plot of changes at various frequencies. Asterisk, $P < 0.001$ vs. I_{Ba}; dagger, $P < 0.001$ vs CaM(WT); both by ANOVA and Bonferroni tests.

© 1999 Macmillan Magazines Ltd

in which mixtures of both were run on non-denaturing polyacrylamide gels (Fig. 5c). With 100 nM Ca^{2+}, which is comparable to the basal Ca^{2+} level in quiescent cells, inclusion of peptide reduced the mobility of CaM. The mobility shift saturated at a peptide:CaM ratio corresponding to a 1:1 complex. In contrast, no shift was found in the absence of Ca^{2+} (data not shown). For comparison, we also tested a peptide from the corresponding region of α_{1B} (N-type channel), which diverged at three positions among the IQ consensus residues (Fig. 5b). This α_{1B}-derived peptide did not alter CaM mobility at either 100 nM (Fig. 5c) or 1 mM free Ca^{2+} (data not shown).

An additional perspective on the CaM-peptide interaction was obtained in fluorescence experiments with dansyl–CaM[20]. The dansyl–CaM emission spectrum displayed an IQ-peptide-dependent blue shift and enhancement, characteristic of a hydrophobic CaM-peptide interaction (Fig. 5d). The apparent K_m for the α_{1C} peptide was 30-fold lower with 2 mM Ca^{2+} than without Ca^{2+}, whereas the α_{1B}-derived peptide displayed only a weak interaction with dansyl–CaM and did not show a Ca^{2+}-dependent increase in affinity (data not shown). The Ca^{2+}-dependence of the dansyl–CaM–α_{1C} peptide interaction (Fig. 5e) was detected as a steep increase in the fluorescence signal over submicromolar Ca^{2+} concentrations. The data were well-fitted by a simple model (see Methods) that allowed different interactions of dansyl–CaM with peptide depending on whether it was complexed with zero, two or four Ca^{2+} ions. Peptide–CaM (P·CaM) binding was favoured by a high-affinity P·CaM–Ca^{2+} interaction ($K_{D1} = 29$ nM), which would give rise to binding at Ca^{2+} levels in quiescent cells (Fig. 5c). However, the main increment in fluorescence arose from a further P·CaM–Ca^{2+} interaction of lower affinity ($K_{D2} = 515$ nM), presumably corresponding to CaM effector action.

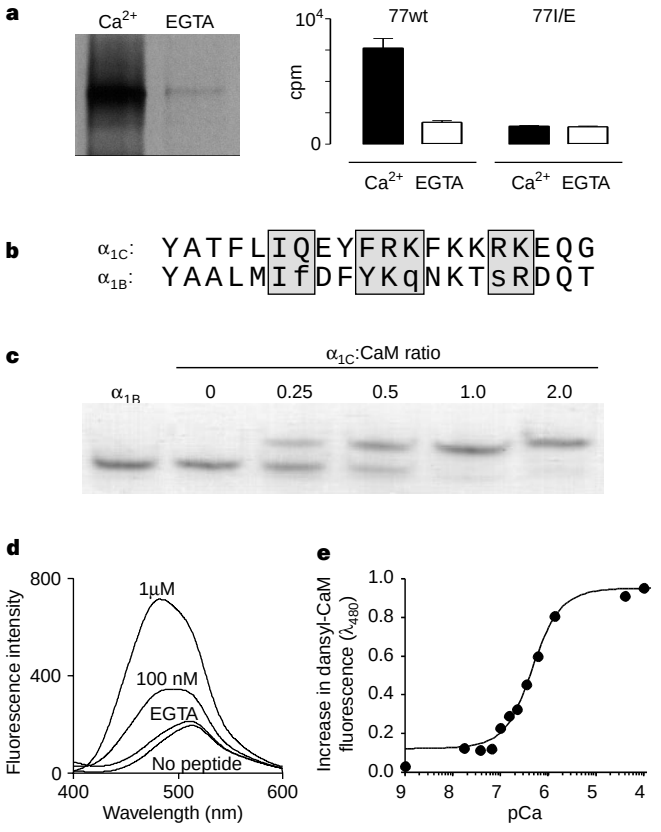

Figure 5 CaM interacts with the IQ motif of α_{1C}. **a**, Left, interaction between CaM and ^{35}S-labelled, *in vitro*-translated α_{1C} C-terminal fragment; right, comparison of wild-type and I/E C-terminal fragments with regard to CaM interaction. **b**, Peptide sequences of consensus IQ region of α_{1C} and corresponding region of α_{1B}. Divergence from consensus indicated in lower case. **c**, Gel mobility-shift assay demonstrating the interaction between CaM and the α_{1C} IQ peptide. CaM was incubated with IQ peptide at the indicated molar ratios in solution containing ~100 nM free [Ca^{2+}]. First lane shows lack of mobility shift with α_{1B} peptide (2:1 ratio over CaM). **d**, Emission fluorescence spectra of dansyl–CaM in the absence (No peptide) or presence of α_{1C} peptide with no added Ca^{2+} (EGTA), 100 nM and 1 μM added Ca^{2+}; spectra have been corrected for background buffer fluorescence. **e**, Ca^{2+}-dependence of peak fluorescence due to interaction between dansyl–CaM (dCaM, 500 nM) and α_{1C} IQ peptide (500 nM). Data points show averages of two independent runs. Smooth curve was derived from a simplified model (Methods) in which dCaM may be complexed with zero, two or four Ca^{2+} ions, either with or without bound IQ peptide. Least-squares fit yielded values of $K_{D1} = 29$ nM, $K_{D2} = 515$ nM.

Our experiments revealed some novel features of L-type-channel gating: first, CaM plays a pivotal role in both Ca^{2+}-dependent inactivation and facilitation; second, a putative IQ motif in the cytoplasmic tail of α_{1C} not only binds CaM but is also important for the opposing modulatory actions; and third, mutation of Ile 1624 to alanine inhibits Ca^{2+}-dependent inactivation and unmasks overt facilitation, whereas its conversion to glutamate eliminates both effects. The involvement of CaM in inactivation had previously been considered[14], but was not substantiated because of the ineffectiveness of calmidazolium[9,14]. This CaM inhibitor would only be expected to block Ca^{2+}-dependent inactivation if CaM acted as a free molecule, but CaM appears to be stably associated with the IQ motif at basal Ca^{2+} levels (Fig. 5c). Such an association may help account for the persistence of Ca^{2+}-dependent inactivation in excised patches[21] and planar bilayers[22]. Overexpression of mutant CaM(3–) exerted a dominant negative effect on inactivation (Fig. 4), but this behaviour only became prominent after expression in oocytes over several days, time presumably needed for turnover and displacement of endogenous CaM. The C-terminal CaM-binding site strategically positions a cytoplasmic Ca^{2+} sensor close to the permeation pathway, favouring local feedback control of channel function. This parallels CaM's involvement in regulating SK channels[19] (in which CaM affects gating by interacting with domains in analogous positions), NMDA channels[23], cyclic-nucleotide-gated cation channels[24] and Ca^{2+} pumps[25]. The L-type Ca^{2+} channel is unusual in using CaM as a regulator of both inactivation and facilitation, which indicates that the same CaM molecule may act as a Ca^{2+} sensor for opposing biological effects. □

Methods

Molecular biology. Site-directed mutagenesis was done using the plasmid p77NB[14] as template. A mutagenic oligonucleotide which introduced the degenerate codon GNA (where N is G, A, T or C) encoding amino-acid residues at position 1,624 was used in PCR reactions. An amplified 400-bp *Van*91I/*Rsa*I-restriction fragment containing the point mutations was subcloned by triple-fragment ligation directly into the plasmid pHLCC77[26], which encodes the full length 77WT-channel subunit. We confirmed the mutations by sequencing the entire 400-bp fragment. *In vitro* transcription of the wild-type and mutant-77 constructs and of the auxiliary constructs $\alpha_2\delta$ (ref. 27) and β_1 (ref. 28) was as described[14]. Transcription of CaM(WT) and CaM(3–)[19] was performed with *Pvu*I-linearized complementary DNA templates and Ambion's T7 mMessage mMachine Kit. The transcription reactions were spiked with 25 units of SP6 RNA polymerase. Isolation and handling of *Xenopus* oocytes followed standard procedures[29]. For co-expression experiments of Ca^{2+} channels with CaM(WT) and CaM(3–), respectively, up to 200 fmol of CaM(WT) and CaM(3–) cRNAs were injected 2–3 days before the injection of Ca^{2+}-channel subunit cRNAs.

Electrophysiology. Whole-cell I_{Ba} and I_{Ca} were recorded in every oocyte by a standard two-electrode voltage clamp method[14]. To eliminate Cl^- currents through endogenous Ca^{2+}-activated channels, we injected 23–46 nl of 100 mM BAPTA (1,2-bis(2-aminophenoxy)ethane-N,N,N′,N′-tetraacetic K_4 hydrate) solution into the oocytes 1–3 h before the recordings. During the recordings, oocytes were superfused with a solution containing (in mM): $Ba(OH)_2$ or $Ca(NO_3)_2$ 40, NaOH 50, KOH 1, HEPES 10 (adjusted to pH 7.4 with

© 1999 Macmillan Magazines Ltd

methanesulphonic acid). Currents were filtered at 0.5 Hz and sampled at 2 Hz, and leak subtraction was performed using an offline P/4 protocol. Data points are mean ± s.e.m.

CaM–α_{1C} interaction. A PCR fragment containing nucleotides 4,710–6,707 was generated from rabbit α_{1C} cDNA and cloned into pCDNA3. Wild-type and I/E sequences were studied. ^{35}S-labelled *in vitro* translated peptide was generated in rabbit reticulocyte lysates, separated from unincorporated ^{35}S by passage over a G50 column, and incubated for 4 h at 4 °C with CaM immobilized on agarose (Calbiochem) in buffer solutions containing 150 mM NaCl, 50 mM Tris–HCl (pH 7.2) plus 0.1% Triton X-100, with either 1 mM $CaCl_2$ or 2 mM EGTA. The CaM-agarose was then washed extensively with the same buffer and the labelled peptide was eluted in SDS, and either quantified by scintillation counting or separated on SDS–PAGE and identified by autoradiography.

Gel mobility-shift assay. CaM (1.5 nmol) was incubated with α_{1C} IQ peptide for 1 h at 22 °C in 50 mM Tris, pH 7.4, 2 μM $CaCl_2$ and 2.5 μM EGTA (calculated free $[Ca^{2+}] \simeq 100$ nM). We subjected the sample to non-denaturing polyacrylamide-gel electrophoresis in the presence of 100 nM free Ca^{2+} before visualizing the CaM complex by staining with Coomassie blue.

Dansyl–CaM studies. Conjugation of highly purified CaM with dansyl (5-dimethyl-aminonaphthalene-1-sulphonyl) chloride (Molecular Probes) was performed for 1 h at room temperature. We purified the product with G-25 Sephadex columns, and carried out binding studies in 150 mM NaCl and 50 mM Tris (pH 7.5), with or without Ca^{2+} as indicated. Fluorescence was monitored with a Perkin-Elmer LS50B luminescence spectrometer with 340 nm excitation. We studied the Ca^{2+}-dependence using a series of Ca^{2+} buffers (Molecular Probes) containing 100 mM KCl, 10 mM MOPS (pH 7.2), 1 mM free Mg^{2+}, and Ca^{2+}-EGTA concentrations adjusted to give the indicated free Ca^{2+}. Mg^{2+} could not functionally substitute for Ca^{2+} in controlling peptide binding (not shown). Peptides were obtained from Research Genetics. The smooth curve describing the fractional increase in fluorescence was derived from a simplified model in which dansyl–CaM (dCaM) may be complexed with 0, 2 or 4 Ca^{2+} ions, either without or with bound IQ peptide (P).

$$\begin{array}{ccccc} \text{P·dCaM} & \leftrightarrow & \text{P·dCaM·2Ca}^{2+} & \leftrightarrow & \text{P·dCaM·4Ca}^{2+} \\ \updownarrow & & \updownarrow & & \updownarrow \\ \text{dCaM} & \leftrightarrow & \text{dCaM·2Ca}^{2+} & \leftrightarrow & \text{dCaM·4Ca}^{2+} \end{array}$$

We assume that occupancy of the dCaM·$2Ca^{2+}$ state is insignificant, because dCaM·$2Ca^{2+}$ would either bind very rapidly to peptide or take on two additional Ca^{2+} ions. Peptide dissociation constants for P·dCaM (10.8 μM) and P·dCaM·$4Ca^{2+}$ (304 nM) were experimentally determined in 0 or 2 mM free Ca^{2+}. P·dCaM ↔ P·dCaM·$2Ca^{2+}$ and P·dCaM·$2Ca^{2+}$ ↔ P·dCaM·$4Ca^{2+}$ reactions were described as 1:1 reactions for simplicity, using $K_{1/2}$ values (K_{D1}, K_{D2}) adjusted by least-squares criterion to fit the experimental data. Calculation of aggregate fluorescence took into account estimates of the relative fluorescence of individual states, dCaM (0.05), P·dCaM (and, by assumption, P·dCaM·$2Ca^{2+}$) (0.229), P·dCaM·$4Ca^{2+}$ (0.657) and dCaM·$4Ca^{2+}$ (0.123).

Received 25 January; accepted 24 March 1999.

1. Bers, D. M. *Excitation–Contraction Coupling and Cardiac Contractile Force* (Kluwer Academic, Dordrecht, 1991).
2. Artalejo, C. R., Adams, M. E. & Fox, A. P. Three types of Ca^{2+} channels trigger secretion with different efficacies in chromaffin cells. *Nature* **367,** 72–76 (1994).
3. Murphy, T. H., Worley, P. F. & Baraban, J. M. L-type voltage-sensitive calcium channels mediate synaptic activation of immediate early genes. *Neuron* **7,** 625–635 (1991).
4. Eckert, R. & Chad, J. E. Inactivation of Ca^{2+} channels. *Prog. Biophys. Mol Biol.* **44**, 215–267 (1984).
5. Noble, S. & Shimoni, Y. The calcium and frequency dependence of the slow inward current 'staircase' in frog atrium. *J. Physiol.* **310,** 57–75 (1981).
6. Gurney, A. M., Charnet, P., Pye, J. M. & Nargeot, J. Augmentation of cardiac calcium current by flash photolysis of intracellular caged-Ca^{2+} molecules. *Nature* **341,** 65–68 (1989).
7. Zygmunt, A. C. & Maylie, J. Stimulation-dependent facilitation of the high threshold calcium current in guinea-pig ventricular myocytes. *J. Physiol.* **428,** 653–671 (1990).
8. McDonald, T. F., Pelzer, S., Trautwein, W. & Pelzer, D. J. Regulation and modulation of calcium channels in cardiac, skeletal, and smooth muscle cells. *Physiol. Rev.* **74,** 365–507 (1994).
9. Imredy, J. P. & Yue, D. T. Mechanism of Ca^{2+}-sensitive inactivation of L-type Ca^{2+} channels. *Neuron* **12,** 1301–1318 (1994).
10. Soldatov, N. M., Zühlke, R. D., Bouron, A. & Reuter, H. Molecular structures involved in L-type calcium channel inactivation. Role of the carboxyl-terminal region encoded by exons 40-42 in α_{1C} subunit in the kinetics and Ca^{2+}-dependence of inactivation. *J. Biol. Chem.* **272,** 3560–3566 (1997).
11. Babitch, J. Channel hands. *Nature* **346,** 321–322 (1990).
12. De Leon, M. *et al.* Essential Ca^{2+}-binding motif for Ca^{2+}-sensitive inactivation of L-type Ca^{2+} channels. *Science* **270,** 1502–1506 (1995).
13. Rhoads, A. R. & Friedberg, F. Sequence motifs for calmodulin recognition. *FASEB J.* **11,** 331–340 (1997).
14. Zühlke, R. D. & Reuter, H. Ca^{2+}-sensitive inactivation of L-type Ca^{2+} channels depends on multiple cytoplasmic amino acid sequences of the α_{1C} subunit. *Proc. Natl Acad. Sci. USA* **95,** 3287–3294 (1998).
15. Zhou, J. M. *et al.* Feedback inhibition of Ca^{2+} channels by Ca^{2+} depends on a short sequence of the C terminus that does not include the Ca^{2+}-binding function of a motif with similarity to Ca^{2+}-binding domains. *Proc. Natl Acad. Sci. USA* **94,** 2301–2305 (1997).
16. Bernatchez, G., Talwar, D. & Parent, L. Mutations in the EF-hand motif impair the inactivation of barium currents of the cardiac α_{1C} channel. *Biophys. J.* **75,** 1727–1739 (1998).
17. Soldatov, N. M. Molecular diversity of L-type Ca^{2+} channel transcripts in human fibroblasts. *Proc. Natl Acad. Sci. USA* **89,** 4628–4632 (1992).
18. Hess, P., Lansman, J. B. & Tsien, R. W. Calcium channel selectivity for divalent and monovalent cations. Voltage and concentration dependence of single channel current in ventricular heart cells. *J. Gen. Physiol.* **88,** 293–319 (1986).
19. Xia, X. M. *et al.* Mechanism of calcium gating in small-conductance calcium-activated potassium channels. *Nature* **395,** 503–507 (1998).
20. Kincaid, R. L., Vaughan, M., Osborne, J. C. Jr & Tkachuk, V. A. Ca^{2+}-dependent interaction of 5-dimethylaminonaphthalene-1-sulfonyl-calmodulin with cyclic nucleotide phosphodiesterase, calcineurin, and troponin I. *J. Biol. chem.* **257,** 10638–10643 (1982).
21. Höfer, G. F. *et al.* Intracellular Ca^{2+} inactivates L-type Ca^{2+} channels with a Hill coefficient of ~1 and an inhibition constant of ~4 μM by reducing channel's open probability. *Biophys. J.* **73,** 1857–1865 (1997).
22. Haack, J. A. & Rosenberg, R. L. Calcium-dependent inactivation of L-type calcium channels in planar lipid bilayers. *Biophys. J.* **66,** 1051–1060 (1994).
23. Zhang, S., Ehlers, M. D., Bernhardt, J. P., Su, C. T. & Huganir, R. L. Calmodulin mediates calcium-dependent inactivation of N-methyl-D-aspartate receptors. *Neuron* **21,** 443–453 (1998).
24. Liu, M., Chen, T., Ahamed, B., Li, J. & Yau, K. W. Calcium-calmodulin modulation of the olfactory cyclic nucleotide-gated cation channel. *Science* **266,** 1348–1354 (1994).
25. Vorherr, T. *et al.* Interaction of calmodulin with the calmodulin binding domain of the plasma membrane Ca^{2+} pump. *Biochemistry* **29,** 355–365 (1990).
26. Soldatov, N. M., Bouron, A. & Reuter, H. Different voltage-dependent inhibition by dihydropyridines of human Ca^{2+} channel splice variants. *J. Biol. Chem.* **270,** 10540–10543 (1995).
27. Singer, D. *et al.* The role of the subunits in the function of the calcium channel. *Science* **253,** 1553–1557 (1991).
28. Ruth, P. *et al.* Primary structure of the β subunit of the DHP-sensitive calcium channel from skeletal muscle. *Science* **245,** 1115–1118 (1989).
29. Zühlke, R. D., Bouron, A., Soldatov, N. M. & Reuter, H. Ca^{2+} channel sensitivity towards the blocker isradipine is affected by alternative splicing of the human α_{1C} subunit gene. *FEBS Lett.* **427,** 220–224 (1998).

Acknowledgements. We thank J. Adelman and J. Maylie for providing CaM(WT) and CaM(−3), C. Klee and M. Ikura for helpful discussions, and H. van Hees for technical assistance. This work was supported by the Swiss National Science Foundation (H.R.), a Pfizer postdoctoral fellowship (G.S.P.), an MSTP training grant (K.D.), and grants from NIH (G.S.P.), NINDS, NIMH, the McKnight Foundation and the Mathers Charitable Trust (R.W.T.).

Correspondence and requests for materials should be addressed to H.R. (e-mail: harald.reuter@pki.unibe.ch).

A cytosolic catalase is needed to extend adult lifespan in *C. elegans daf-C* and *clk-1* mutants

James Taub*†, Joe F. Lau*, Charles Ma*, Jang Hee Hahn*‡, Rafaz Hoque*, Jonathan Rothblatt*† & Martin Chalfie*

** Department of Biological Sciences, Columbia University, 1212 Amsterdam Avenue, New York, New York 10027, USA*
† Department of Biological Sciences, 6044 Gilman Laboratory, Dartmouth College, Hanover, New Hampshire 03755, USA

The dauer larva is an alternative larval stage in *Caenorhabditis elegans* which allows animals to survive through periods of low food availability. Well-fed worms live for about three weeks, but dauer larvae can live for at least two months without affecting post-dauer lifespan[1]. Mutations in *daf-2* and *age-1*, which produce a dauer constitutive (Daf-C) phenotype, and in *clk-1*, which are believed to slow metabolism, markedly increase adult lifespan[2]. Here we show that a *ctl-1* mutation reduces adult lifespan in otherwise wild-type animals and eliminates the *daf-c* and *clk-1*-mediated extension of adult lifespan. *ctl-1* encodes an unusual cytosolic catalase; a second gene, *ctl-2*, encodes a peroxisomal catalase. *ctl-1* messenger RNA is increased in dauer larvae and adults with the *daf-c* mutations. We suggest that the *ctl-1* catalase is needed during periods of starvation, as in the dauer larva, and that its misexpression in *daf-c* and *clk-1* adults extends lifespan. Cytosolic catalase may have evolved to protect nematodes from

‡ Present addresses: Department of Anatomy, College of Medicine, Kangwon National University, Chunchon, 200-701, Korea (J.H.H.); Center for Applied Genomics, Hoechst Marion Roussel, Fraunhoferstr. 22, 82152 Martinsried, Germany (J.R.).

© 1999 Macmillan Magazines Ltd